Lateral Diffusion of an Integral Membrane Protein: Monte Carlo Analysis of the Migration of Phosphorylated Light-Harvesting Complex II in the Thylakoid Membrane†

Friedel Drepper,‡ Inger Carlberg,§ Bertil Andersson,§ and Wolfgang Haehnel*,‡

Lehrstuhl für Biochemie der Pflanzen, Albert-Ludwigs-Universität, Schänzlestrasse 1, D-79104 Freiburg, Germany, and Department of Biochemistry, Arrhenius Laboratories for Natural Sciences, Stockholm University, S-10691 Stockholm, Sweden

Received May 18, 1993; Revised Manuscript Received August 9, 1993®

ABSTRACT: The lateral migration of the integral light-harvesting chlorophyll *a/b* protein complex of photosystem II, LHCII, has been studied in the undisturbed membranes of thylakoids without artificial probes. LHCII was phosphorylated at 0 °C. The diffusion of the mobile phospho-LHCII from appressed grana to nonappressed membrane regions was induced by a temperature jump to 20 °C and analyzed by a rapid detergent fractionation of the two membrane areas. This long-range diffusion of the integral phospho-LHCII is analyzed by a Monte Carlo calculation which is based on a model of the thylakoid membrane and includes all integral proteins as mobile particles. A comparison of the calculation with the experimental time course indicates a diffusion constant of phospho-LHCII in the range of (2–4) × 10^{-12} cm^2 s^{-1}. This value is evidence for a severe restriction of protein mobility in the appressed thylakoid membrane. From a statical point of view, the percolation theory predicts that the high protein density in the grana membranes is above the threshold of percolation and the long–range diffusion should be inhibited by finite clusters of lipids. However, the shape of the experimental time course is in favor of a lateral motion also of photosystem II and nonphosphorylated LHCII and not of a rigid lattice of these complexes. Our data and Monte Carlo analysis suggest a dynamic or fluid lattice of the protein complexes with a lifetime of the clusters in the millisecond time range. The consequences of these transient fluctuations on the long-range diffusion of plastoquinone are discussed.

Lateral migration of integral proteins is a basic feature of membrane function, regulation, and biosynthesis. For the function and acclimation of the photosynthetic apparatus in plants, the lateral transport of proteins or protein complexes between the stroma-exposed and the appressed regions of the thylakoid membrane system is an essential process (Andersson & Styring, 1991). Of special importance is the transport of newly synthesized photosystem II (PS II)[1] subunits from the stroma-exposed to the appressed membrane regions during biosynthesis and assembly of PS II (Mattoo & Edelman, 1987; Yalovsky et al., 1989), lateral migration of PS II subunits in connection with the high turnover of D1 reaction center protein (Adir et al., 1990; Hundal et al., 1990), and rearrangement of the light-harvesting chlorophyll *a/b* protein complex of photosystem II, (LHCII) during light and heat stress (Anderson & Andersson, 1988). More recently, evidence has been accumulated to suggest a controlled lateral migration of the cytochrome *bf* complex related to the state 1 → state 2 transition (Vallon et al., 1991) that may well be induced by phosphorylation (Gal et al., 1992). The separation of the two membrane regions under various metabolic or biosynthetic conditions provides the possibility to study the lateral diffusion in this native biological membrane without addition of various probes. An experimental approach to these problems is provided by the light-induced phosphorylation of LHCII which is regarded as an essential mechanism for the regulation of the energy distribution between the two photosystems in plants (Allen et al., 1981; Allen, 1992). The reaction is catalyzed by a membrane-bound kinase and controlled by the redox state of the plastoquinone pool (Horton et al., 1981) and the cytochrome *bf* complex (Gal et al., 1987). The dissociation of a mobile subpopulation of the phospho-LHCII from PS II and its subsequent lateral migration from the appressed grana membranes to the PS I containing stroma-exposed membranes (Kyle et al., 1983; Andersson et al., 1982; Larsson & Andersson, 1985) have been suggested to be important for balancing the excitation energy and protection against photodestruction of PS II (Anderson & Andersson, 1988; Allen, 1992; Barber, 1982).

Recent results have shown that the protein kinase is still active and phosphorylates LHCII at temperatures as low as 0 °C but that the lateral movement of the mobile phospho-LHCII is virtually impaired at these temperatures (Carlberg et al., 1992). A subsequent rapid increase of the temperature induces the diffusion of the phospho-LHCII from appressed grana to nonappressed membrane regions which can be followed by fractionation of the membranes (Carlberg et al., 1992). This possibility to start the migration of LHCII after its phosphorylation has been completed allows the study and modeling of the actual diffusional process within the thylakoid membrane.

Monte Carlo Method. The diffusion equation cannot be solved for complex boundary conditions as found in biological membranes. However, the Monte Carlo method introduced by Metropolis et al. (1953) to investigate properties of

† This work was supported by the Deutsche Forschungsgemeinschaft (SFB 171-A3), by the Swedish Natural Science Research Council, and by the Swedish Council for Forestry and Agricultural Research.

* Correspondence should be addressed to this author.
‡ Albert-Ludwigs-Universität.
§ Stockholm University.

® Abstract published in *Advance ACS Abstracts,* October 15, 1993.

[1] Abbreviations: FRAP, fluorescence recovery after photobleaching; LHCII, light-harvesting chlorophyll *a/b* protein complex of photosystem II; PS, photosystem; SDS–PAGE, sodium dodecyl sulfate–polyacrylamide gel electrophoresis; Tricine, *N*-[tris(hydroxymethyl)methyl]glycine.

0006-2960/93/0432-11915$04.00/0

interacting individual molecules in terms of a rigid-sphere system can provide a numerical solution. The Monte Carlo algorithm has been used to simulate a broad range of complex systems (Binder, 1987) including protein folding (Li & Scherga, 1987). Generally one starts from a description of a system in terms of a model. Random numbers are used to create a Markov chain of new states. In detail, in a simulation of membrane diffusion an object is moved across an incremental distance in a randomly selected direction. This is calculated sequentially for all mobile objects to give a new configuration. If subsequent configurations can be related to a time-scale, the result represents a solution of the diffusion equation for the complex boundary conditions defined in the model. In our calculation of the individual Monte Carlo steps, a hard-sphere reflection is included in the movement if an encounter with a boundary of another object occurs. Besides this algorithm, most important for the diffusion are the size and the density of the integral complexes. Above a membrane fraction of about 0.5 being occupied by obstacles, there is no continuous path through an extended area of the membrane (Saxton, 1987). This limit of percolation has been discussed as an important parameter for the diffusion of small lipid molecules as plastoquinone and ubiquinone as well as for integral proteins. Such an obstruction of the diffusion by high protein density may result in a considerable difference between the actual microscopic diffusion coefficient and the macroscopic diffusion coefficient important for long-range effects.

In a previous study (Mitchell et al., 1990), a possible obstruction of plastoquinol diffusion within its reaction sequence in linear photosynthetic electron transport was analyzed by a Monte Carlo approach. Recently it was suggested that the hindrance by integral proteins could severely restrict the long-range diffusion of plastoquinone (Joliot et al., 1992). In order to analyze the diffusion of the integral phospho-LHCII, we have now expanded our model of the thylakoid membrane by including all integral proteins as mobile particles in the Monte Carlo approach. A comparison of the model calculation with the diffusion kinetics of the phospho-LHCII is used to estimate the diffusion constants of the complexes in the intact thylakoid membrane. On the basis of the estimation of LHCII migration, we have also analyzed the lateral diffusion of plastoquinol taking into account the archipelago effect of mobile protein complexes and the lifetime of isolated clusters of lipid area.

MATERIALS AND METHODS

Kinetic Subfractionation of Phosphorylated Thylakoid Membranes. From spinach grown as described in Carlberg et al. (1992), thylakoids were isolated according to Andersson et al. (1976). The protein phosphorylation and "kinetic" subfractionation were done as previously described (Carlberg et al., 1992) and detailed below. Thylakoids were phosphorylated at a chlorophyll concentration of 0.4 mg/mL by 10-min illumination (500 μmol of photons m^{-2} s^{-1}) at 0 °C in the presence of 0.4 mM [γ-^{32}P]ATP in 50 mM Tricine–KOH, pH 7.6, 20 mM NaCl, 5 mM $MgCl_2$, 0.1 M sorbitol, and 10 mM NaF (incubation medium). Subsequent to the phosphorylation, the thylakoids were moved to darkness and a temperature of 20 °C. This was done by transferring the sample to a wide beaker in a water bath kept at 20 °C, thus allowing for a large contact area between the sample and the temperature bath. The total manipulation time before the start of the migration studies was 1.5–2 min, which was found to be sufficient for the sample to equilibrate to 20 °C. At specified time points, samples were withdrawn and fractionated into stroma thylakoid membranes and the rest of the thylakoid membrane system by incubation with digitonin (0.2% w/w per milligram of chlorophyll) for 15 s. The fractionation was stopped by a 10-fold dilution with incubation medium, and the stroma thylakoid membranes were collected after differential centrifugation at 100000*g* (Carlberg et al., 1992). The

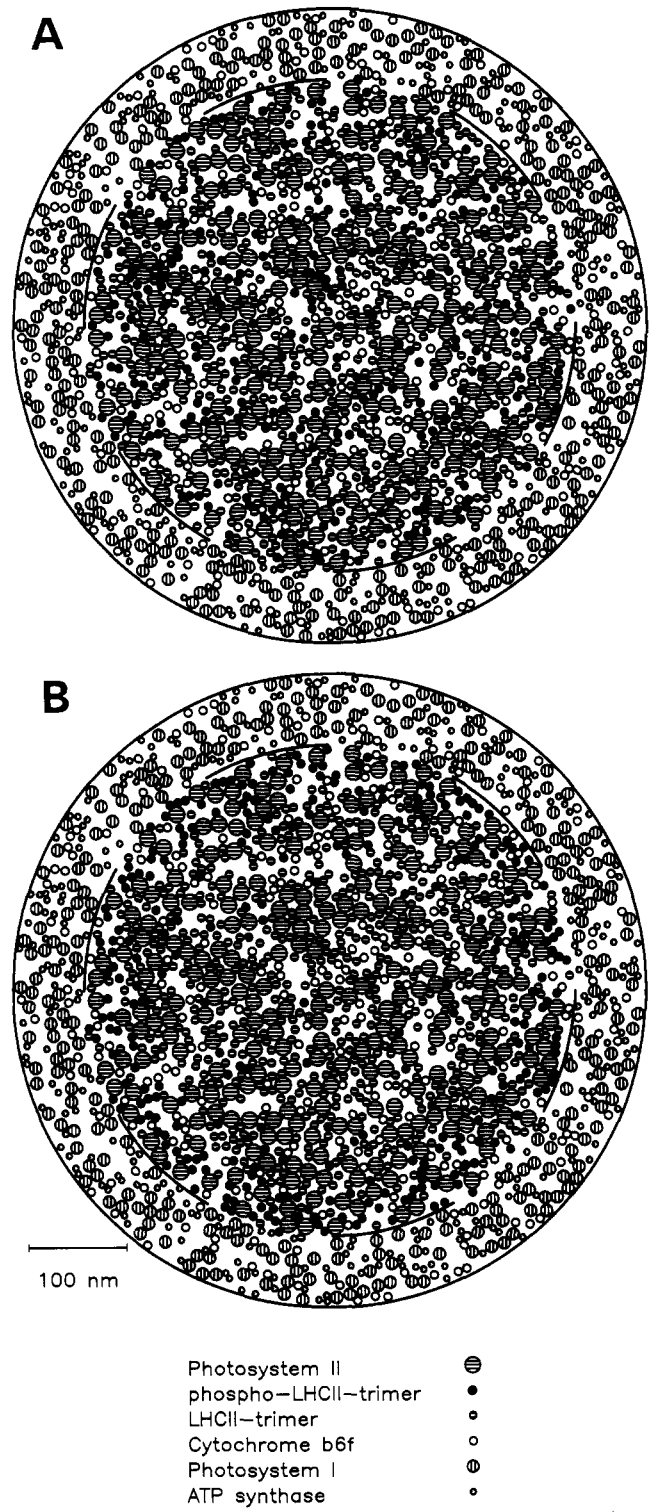

FIGURE 1: (A) Model of the lateral heterogeneity of the thylakoid membrane. The area inside and outside the broken circle represents the appressed grana and the nonappressed membrane region, respectively. This map is used as the starting condition for the Monte Carlo simulation with phospho-LHCII (filled circles) homogeneously distributed in the granum. (B) Alternative starting condition with LHCII being preferentially phosphorylated near the edge of the granum. The number of phospho-LHCII inside successive ring-shaped areas of 40-nm width starting from the edge of the granum are 172, 70, 13, 13, 2, and 1.

Table I: Assumptions for Particles in the Thylakoid Model

particle	diameter (nm)	density (particles/μm^2)	number
PS II	16.0[a]	1380	271
phospho-LHCII trimer	7.4[c]	1380[b]	271
LHCII trimer	7.4[c]	2760[b]	542
cytochrome *bf*	8.0	828[b]	271
PS I	12.0	2093	274
ATP synthase	6.0	2024	265

[a] PS II with bound LHCII. [b] Total of 4920 particles/μm^2 with about 8 nm in diameter consistent with 3 mobile LHCII trimers and 0.6 cytochrome *bf* complex per photosystem II (Staehelin, 1986). [c] Kühlbrandt and Wang (1991).

relative content of phospho-LHCII in the isolated stroma-exposed thylakoids was analyzed on SDS–PAGE using a 12–22% polyacrylamide gradient in the separation gel. The gels were stained and autoradiographed. The films were analyzed by laser densitometry for quantification.

Model of Thylakoid Membrane Organization. The model of the stacked thylakoid membrane used for the Monte Carlo calculations is shown in Figure 1. It is considerably developed as compared to our previous model (Mitchell et al., 1990) in order to simulate the diffusion of the integral complexes. Figure 1A,B is based on identical assumptions on the membrane organization and differ only in the initial distribution of phospho-LHCII as detailed below. The area in the center inside the broken circle represents the appressed region of a granum with 60% of the total area and a diameter of 500 nm; 50% of the circumference of the granum connects to the area outside that represents the nonappressed stroma-exposed region. The values were estimated from electron micrographs of spinach thylakoids taken from the same batch as those used for the experiments (not shown). The randomly distributed small circles with different diameters represent the integral protein complexes of the photosynthetic membrane as given in the legend of Figure 1. PS II complexes are located only in the appressed region, and PS I and ATPase complexes are restricted to the stromal region, while the density of the cytochrome *bf* complex is assumed to be virtually the same within the two regions (Anderson & Andersson, 1988). PS II is closely associated with a discrete number of LHCII which increase its size observed in electron microscopy from 8.3 to 16 nm (Armond et al., 1977). This difference in size is attributed to about nine LHCII which may be attached to PS II in a circular arrangement as suggested for LHCI and PS I (Boekema et al., 1990). In addition to the PS II complexes with bound LHCII (Armond et al., 1977), we assume three mobile LHCII trimers per PS II within the appressed region to account for the total number of 8-nm particles observed in the protoplasmic fracture face of electron micrographs (Staehelin, 1986; Kyle et al., 1983) as well as for the total antenna size of PS II (Andersson & Styring, 1991). A diameter of about 8 nm is consistent with that of a LHCII trimer determined by electron crystallography (Kühlbrandt & Wang, 1991). Table I lists the particle density and the diameter of all complexes used in the calculations. The values are consistent with the data from freeze–fracture experiments [*cf.* Haehnel (1984)]. These assumptions result in 50% of the appressed grana membranes being occupied by integral proteins. Within the grana and stroma-exposed region, respectively, the particles are randomly distributed.

Starting Condition of Phospho-LHCII Diffusion. About one LHCII per PS II is assumed to be phosphorylated during the illumination period preceding the diffusion. For the initial distribution of these phosphorylated LHCII complexes, two different possibilities have been considered. One is a homogeneous distribution in the appressed grana region as shown in Figure 1A. An alternative distribution is suggested by the immunogold labeling of the protein kinase which seems to be preferentially located close to the edge of the grana (Gal et al., 1990; Yu et al., 1992). If the mobility of phospho-LHCII is negligible at 0 °C (Carlberg et al., 1992), the initial distribution of phospho-LHCII should be the same as that given for the kinase (Figure 1B). To model the results of the immunogold labeling of the kinase as close as possible, we have classified the granal areas into rings of 40-nm width starting from the outer border based on the original data (Gal and Ohad, unpublished results; Gal et al., 1990). The total number of phospho-LHCII is the same both in Figure 1A and in Figure 1B.

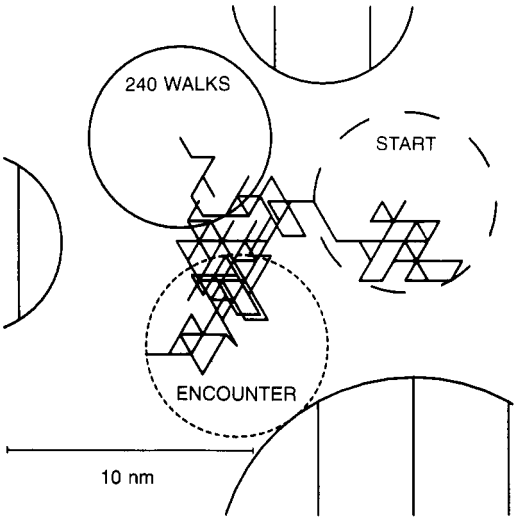

FIGURE 2: Expanded part of the map in Figure 1A. Diffusion path of the LHCII molecule as generated by the Monte Carlo algorithm. The starting position of the simulation is labeled by a dashed circle. On encounter with another complex, a hard-sphere reflection is simulated (dotted circle). For the sake of simplicity in this simulation, the diffusion of one single LHCII molecule was calculated, while the other complexes remained fixed.

Monte Carlo Algorithm. The diffusion of a system with the given complex boundary conditions can only be solved by the Monte Carlo algorithm. In each iteration (termed "walk"), all complexes are moved by 1 nm, corresponding approximately to the distance between lipid molecules in the membrane. This movement took place in one of six randomly selected directions spaced at 60° intervals. In improving previous calculations, we introduce hard-sphere collisions. This is shown in Figure 2 for a random walk of a single complex. The position of the complex on the encounter of another complex is indicated by the dotted circle. On that encounter of the complex, its movement continues in the direction of the angle of a hard-sphere reflection until it has travelled the full distance of 1 nm. In that way, the position after the reflection is different from a point of the trigonal lattice given by the movement before the encounter. This results in a random width of the gaps between the complexes and is important for a simulation of the diffusion of LHCII and in particular of small molecules such as plastoquinone obstructed by these complexes.

For complexes which differ in their diameter, the diffusion coefficients are proportional to the reciprocal of the diameter. In the appressed region, there are only the PS II complexes with the diameter a factor of 2 larger than that of the other complexes with a diameter of about 8 nm (Table I). Therefore, $D_{PSII} = 0.5D_{LHC}$ is assumed for PS II. In the Monte Carlo approach, we have modeled the different diffusion coefficients for individual complexes by reducing the number of random

walks of these complexes relative to that of phospho-LHCII. A complex i is moved only in every n_ith walk given by the nearest integer n_i of the ratio of $D_{p\text{-}LHC}$ and its diffusion coefficient D_i:

$$n_i = D_{p\text{-}LHC}/D_i \quad (1)$$

where i denotes the grana particle different from phospho-LHCII, i.e., LHCII (nonphosphorylated), PS II, and the cytochrome *bf* complex.

Besides the diameter, the interaction between the integral complexes may affect their lateral diffusion. In the appressed grana membranes, it is in particular the attraction between LHCII complexes of adjacent membranes which is responsible for this organization and should restrict their diffusion. Within a grana membrane, LHCII may also be tightly associated with neighboring LHCII and PS II, although LHCII appears as individual particles in freeze–fracture electron micrographs (Kyle et al., 1983). In a first approximation, we have included these interactions into our model by an increased mobility of phospho-LHCII relative to that of LHCII and PS II with associated LHCII by a variable ratio n_i of the diffusion coefficients according to eq 1. For the cytochrome *bf* complex as well as for phospho-LHCII, there is no evidence for this type of attraction, and their diffusion coefficients are assumed to be equal, $D_{BF} = D_{p\text{-}LHC}$.

Further details of the Monte Carlo algorithm are as follows: (i) On encounter of a complex with the boundary between the grana and the stroma regions (Figure 1) one of the other possible directions for movement of the complex is selected. (ii) At the boundary of a granum, only phospho-LHCII is allowed to escape through the openings to the stroma region. Other complexes are considered to be restricted to the appressed region. (iii) The migration of LHCII from stroma back to grana membranes is assumed to be negligible. Thus, when phospho-LHCII has reached the stroma membrane region, the number of phospho-LHCII in the stroma is increased by 1. The output of the model is the fraction of the total phospho-LHCII that has reached the stroma membrane as a function of the number of walks. (iv) Finally, this output is fitted by a least-squares method to the fraction of total phospho-LHCII in the nonappressed stroma regions found as a function of time after the rapid subfractionation of the membranes. The time (t) per walk is given by

$$t = X^2/4D \quad (2)$$

where X is the step length of 1 nm and D is the diffusion coefficient in the lipid bilayer without hindrance. By using eq 2, the best fit gives the diffusion coefficient of phospho-LHCII. The diffusion coefficient of the other complexes is determined by eq 1.

Simulations. The Monte Carlo simulations were written in FORTRAN77 and carried out on a minicomputer (A700; Hewlett-Packard) with a vector processor card. The library routine of the random number generator was tested for uniformity of distribution. The program allows interactive selection of all structural parameters of the membrane model under graphic control.

RESULTS

Migration of Phosphorylated Light-Harvesting Complex. An experimental goal of this study was to measure the time course of the phospho-LHCII diffusion with improved accuracy as compared to the previous data (Carlberg et al., 1992). Figure 3 presents data from five independent subfractionation experiments in which the relative amount of phospho-LHCII appearing in the stroma-exposed thylakoids after transfer from 0 to 20 °C was measured at specified time points. The experiments show that 40–50% of the migrating population has appeared in the stroma membranes already after 2 min and that after 10–15 min no further migration occurs. This lateral migration after phosphorylation in the light is specific for the outer LHCII subpopulation enriched in the 25-kDa subunit (Larsson & Andersson, 1985; Carlberg et al., 1992). The data are normalized to the maximum of the relative amount of phospho-LHCII found in the stroma thylakoid fraction after 17 min. These normalized data are used as a reference for all Monte Carlo simulations. The quality of the fit of the calculated data is given by χ^2, which is proportional to the sum of the least squares of the deviation from the experimental data points.

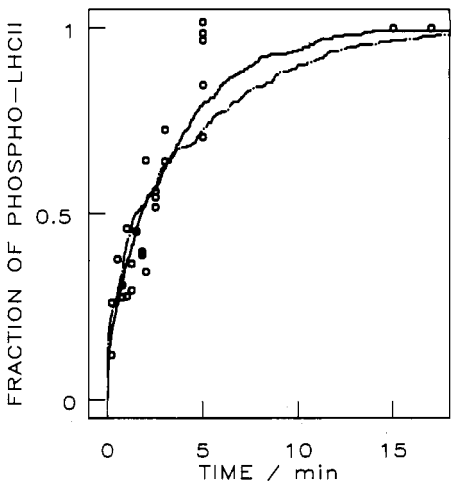

FIGURE 3: Fit of the Monte Carlo calculation to data from rapid subfractionation experiments at ratios $D_{p\text{-}LHC}/D_{LHC}$ of 1 (continuous line) and 500 (broken line), giving diffusion coefficients of 1.9×10^{-12} cm^2 s^{-1} ($\chi^2 = 0.267$) and 2.5×10^{-11} cm^2 s^{-1} ($\chi^2 = 0.408$), respectively. The output of the model is shown as the fraction of total phospho-LHCII that has reached the stroma region. The amount of ^{32}P-LHCII in the stroma fraction as a function of time at 20 °C is shown (circles). χ^2 is the sum of the squared residuals.

For a homogeneous starting distribution of phospho-LHCII within the appressed grana region (Figure 1A), the same mobility was initially assumed for both LHCII and phospho-LHCII; i.e., the diffusion coefficient of LHCII is not changed after phosphorylation except that the phospho-LHCII would leave the grana region at the open boundary toward the stroma region. The diffusion coefficient derived from the best fit represented by the continuous line in Figure 3 is $D_{p\text{-}LHC} = 1.9 \times 10^{-12}$ cm^2 s^{-1}. However, strong interactions between LHCII in adjacent appressed membranes and lateral interactions may considerably restrict the mobility of LHCII. The modification of LHCII by the negatively charged phospho group is likely to decrease both of these interactions and could result in faster diffusion of phospho-LHCII as compared to LHCII. We have modeled this effect by assuming a ratio of the diffusion coefficients $D_{p\text{-}LHC}/D_{LHC}$ ranging from 1 to 500 in the Monte Carlo simulation. The diffusion coefficient $D_{p\text{-}LHC}$ derived from the best fit of each simulation is given in Table II as well as the related diffusion coefficient of nonphosphorylated LHCII. This illustrates that hindrance of phospho-LHCII movement by the other integral complexes being relatively immobile is compensated by faster diffusion of LHCII induced by its phosphorylation. For example, when the diffusion of LHCII is 10-fold slower than that of phospho-LHCII, the diffusion coefficient of phospho-LHCII increases by a factor

Table II: Comparison of Results for Different Model Assumptions[a]

initial distribution of p-LHCII in grana	$D_{p\text{-}LHC}/D_{LHC}$	$D_{p\text{-}LHC}$ ($cm^2\ s^{-1}$)	D_{LHC} ($cm^2\ s^{-1}$)	χ^2
homogeneous	1	1.9×10^{-12}	1.9×10^{-12}	0.267
	10	4.4×10^{-12}	4.4×10^{-13}	0.308
	100	1.1×10^{-11}	1.1×10^{-13}	0.329
	500	2.5×10^{-11}	5.0×10^{-14}	0.408
enriched near grana edge	1	0.84×10^{-12}	0.84×10^{-12}	0.457
	10	0.82×10^{-12}	0.82×10^{-13}	0.731

[a] χ^2 is the sum of the squared residuals; $D_{p\text{-}LHC}$ and D_{LHC} are the diffusion coefficients of phosphorylated and nonphosphorylated LHCII. Assumptions: $D_{PSII} = 0.5D_{LHC}$; $D_{BF} = D_{p\text{-}LHC}$.

of 2.4 as compared to that at equal diffusion coefficients. However, at an increasing ratio of the diffusion coefficients, the deviation of the Monte Carlo simulation from the experimental data increases as indicated by the value of χ^2 in Table II. Moreover, in contrast to a ratio of $D_{p\text{-}LHC}/D_{LHC}$ between 1 and 10 at the extreme ratio of 500, the appearance of phospho-LHCII in the stroma-exposed membranes shows a biphasic time course that is not consistent with the experimental data (broken line in Figure 3).

Alternatively to a homogeneous initial distribution of phospho-LHCII in the appressed grana region, we have also considered as a starting condition for the Monte Carlo calculation phospho-LHCII preferentially located close to the grana margins (Figure 1B) as reported for the membrane-bound kinase (Gal et al., 1990). The broken line in Figure 4 shows the best fit of this simulation at $D_{p\text{-}LHC} = D_{LHC}$ with a derived diffusion coefficient of $D_{p\text{-}LHC} = 0.84 \times 10^{-12}$ $cm^2\ s^{-1}$ (see Table II). The smaller value as compared to that found with the homogeneous initial distribution of phospho-LHCII reflects the shorter distance that most of the phospho-LHCII have to diffuse before reaching the stroma-exposed membrane. However, a few phospho-LHCII have to diffuse from the central region of the appressed area and appear significantly later in the stroma region, leading to clearly biphasic kinetics (Figure 4). This is not consistent with the experimental data. A Monte Carlo simulation with this edge-enriched initial distribution of phospho-LHCII assuming a slower diffusion of nonphosphorylated LHCII and PS II relative to phospho-LHCII results in an even more pronounced biphasic time course than that in Figure 4, broken line (not shown), as indicated by the high value of χ^2 in Table II.

Archipelago Effect and Plastoquinone Diffusion. The data in Figures 3 and 4 provide information about the movement of integral protein complexes. The Monte Carlo analysis extended to all complexes in the granum led us to analyze the random formation and lifetimes of clusters of complexes which could trap plastoquinol molecules and restrict their diffusion (Lavergne & Joliot, 1991). This effect is termed the archipelago effect (Saxton, 1987). Critical parameters for this effect are the particle density and the width of a gap necessary for the trapped molecule to pass. Our simulation of hard-sphere collisions (Figure 2) results in a random distance of all complexes, which is a considerable improvement over fixed positions for an analysis of the archipelago effect in particular on the diffusion of small molecules trapped by large complexes. As a first approximation, we assume that plastoquinol can pass through gaps ≥3 nm between complexes. To analyze a given distribution of the complexes for clusters which would trap plastoquinol, we increased the radii of all complexes by 1.5 nm as shown in an expanded plot of the granal part of the thylakoid model in Figure 5. In this way, any gap wider than 3 nm is easily recognized, and a possible pathway for the rapidly diffusing plastoquinol can be identified. We selected a PS II and determined the region of lipid area

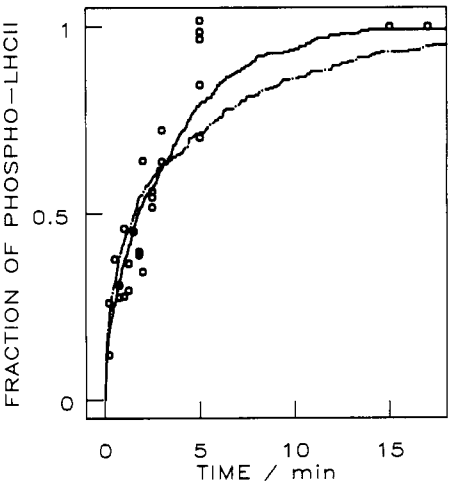

FIGURE 4: Equivalent to Figure 3, but with the output from the model as a function of the initial distribution of phospho-LHCII. Homogeneous distribution (continuous line, same as in Figure 3); enriched concentration at grana edge (broken line, $\chi^2 = 0.457$).

that is in contact with one-fourth of the surface of this particular complex, which is taken as a representation of the plastoquinone binding site. This isolated region, shown as a filled area in Figure 5A, is accessible to a plastoquinol molecule released from the quinone binding site of PS II. In a computer analysis, we determined after every walk the area which had become directly or indirectly accessible to this initially isolated region. This procedure accounts for the high experimental value of the plastoquinone diffusion constant between 10^{-8} and 3×10^{-9} $cm^2\ s^{-1}$ (Millner & Barber, 1984; Cramer et al., 1991), which is larger than the $D_{p\text{-}LHC}$ value by a factor of 1.5 $\times 10^3$ to 5×10^3. The extent of this area representing the propagation of plastoquinol after 25 and 50 walks is shown as a hatched area in Figure 5B and Figure 5C, respectively. The equivalent time to a given number of walks is calculated from the diffusion coefficient (eq 2). At a diffusion coefficient of $D_{p\text{-}LHC} = 1.9 \times 10^{-12}$ $cm^2\ s^{-1}$ (*cf.* Figure 3 and Table II), 50 walks are equivalent to 70 ms. Figure 5A,B,C shows in black clusters complexes separating isolated areas of lipids as discussed by Joliot et al. (1992). However, the possible hindrance of plastoquinol diffusion strongly depends on the complex mobilities and is estimated from the Monte Carlo simulation. The lifetime of the isolated lipid areas was found to be typically equivalent to 7 walks.

DISCUSSION

The diffusion of phosphorylated LHCII in the thylakoid membrane has been studied by following the kinetics of its appearance in the nonappressed membrane region. For an analysis of the experimental data, a structural model of the thylakoid membrane has been built taking into account the dimension of the integral complexes, their density in the appressed and nonappressed membrane regions, and their relative mobility. The diffusion within this multicomponent system is solved by a Monte Carlo approach. A fit of the Monte Carlo simulation to the experimental data gives the value of the diffusion coefficient of the complexes in the intact thylakoid membrane. Assuming in a first approximation equal diffusion coefficients for phospho-LHCII and nonphosphorylated LHCII, we found a value for the microscopic diffusion coefficient $D_{p\text{-}LHC}$ of 1.9×10^{-12} $cm^2\ s^{-1}$. This value is about 2 orders of magnitude lower than that reported for membrane proteins of similar size in artificial lipid bilayers (Blackwell et al., 1987; Gupte et al., 1984). Gupte et al. (1984), using fluorescence recovery after photobleaching (FRAP), deter-

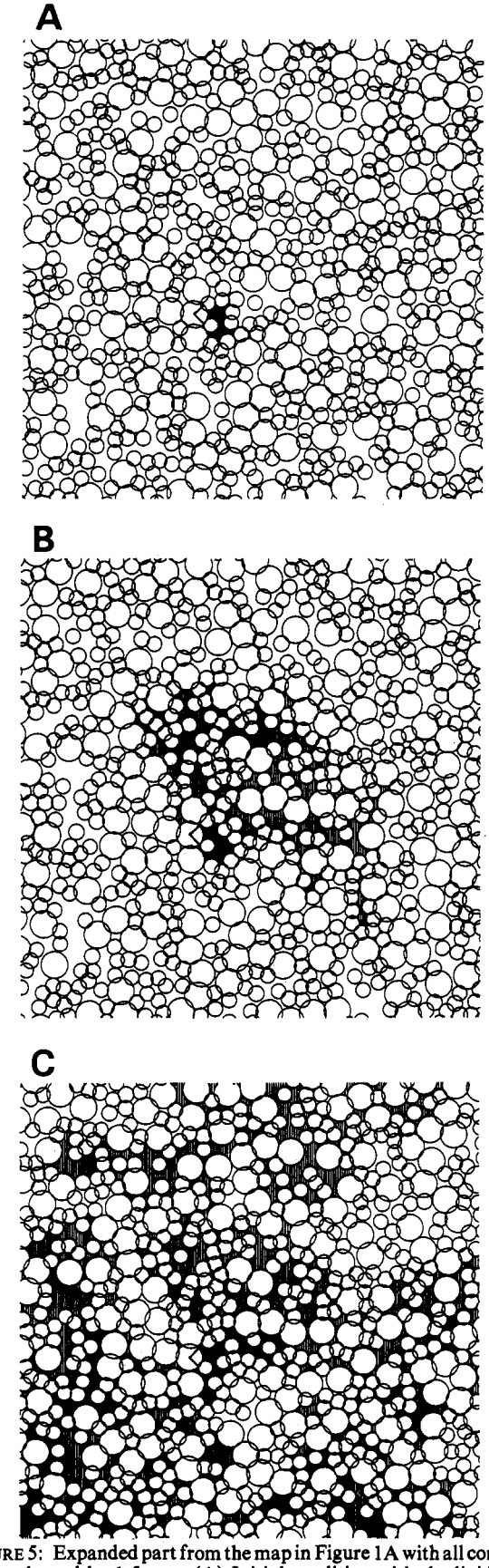

FIGURE 5: Expanded part from the map in Figure 1A with all complex radii enlarged by 1.5 nm. (A) Initial condition with the lipid area in contact with a plastoquinone binding site of one PS II indicated (filled area). (B) Same membrane region as in (A) after 25 Monte Carlo steps of 1 nm per particle. The region that has been found in direct and indirect contact with the original cluster in (A) after all intermediate walks is also indicated (hatched area). (C) Equivalent to (B) after 50 Monte Carlo steps per LHCII. The hatched area is accessible to plastoquinol released by the marked PS II in (A) if it diffuses fast in comparison to the integral proteins.

mined the diffusion coefficient of the mitochondrial cytochrome *bc* complex as 4×10^{-10} cm^2 s^{-1}. FRAP monitors the macroscopic diffusion. For a diffusional process that is obstructed by clusters of obstacles, the diffusion coefficient derived from the macroscopic observation is even smaller than the actual microscopic diffusion coefficient. Therefore, the very small microscopic diffusion coefficient derived by the Monte Carlo analysis from our experimental data indicates a strong restriction of the diffusion of phospho-LHCII. This is consistent with the strong interaction between LHCII molecules in adjacent appressed membranes and the energy transfer between these complexes (Trissl et al., 1987) as well as in the same appressed membrane. The macroscopic diffusion coefficient of phospho-LHCII can be estimated from the half time of 2 min in Figure 3. The average distance for phospho-LHCII to reach the circular boundary of the granum is one-sixth of the diameter of 500 nm, i.e., 83 nm. Thus, eq 2 gives a macroscopic or long-range diffusion coefficient of 1.4×10^{-13} cm^2 s^{-1}, which is an order of magnitude smaller than the value of the actual one. This is consistent with the idea of a distance-dependent diffusion coefficient in membranes with a high density of obstacles which has been used to account for observations of the same object but by techniques covering different periods of time (Saxton, 1987, 1992).

In a different approach to the diffusion of the integral complexes, Rubin et al. (1981) studied the restacking of thylakoid membranes after addition of $MgCl_2$. These authors monitored the change of chlorophyll fluorescence which is related to the association of nonphosphorylated LHCII with PS II. In contrast to the situation after LHCII phosphorylation, this process includes the motion of all components during the lateral redistribution and the forming of membrane–membrane interactions. The measurements gave an effective macroscopic diffusion coefficient of $D = 6 \times 10^{-12}$ cm^2 s^{-1} at 20 °C (Rubin et al., 1981). Our value being lower by more than an order of magnitude indicates that the diffusion in the appressed membranes is severely restricted as compared to destacked thylakoid membranes.

An important aspect of the diffusional mechanism and the regulation of energy conversion is the question of whether the energy transfer from LHCII to PS II is interrupted simultaneously with (i) its phosphorylatioin, (ii) the start of the lateral diffusion, or (iii) the transfer of phospho-LHCII to nonappressed membrane regions. An interruption of energy transfer from a fraction of total LHCII to PS II would decrease the cross section of the PS II antennae. This can be detected by a decrease of the rate of oxygen evolution at limiting light intensities. Previous experiments with thylakoids indicate that the rate of oxygen evolution at limiting light intensity does not decrease during the phosphorylation at 0 °C (Carlberg et al., 1992). Further preliminary experiments (not shown) indicate that after transfer to 20 °C a decrease of the oxygen evolution rate is complete within 30 s. This is evidence that the energy transfer to PS II is interrupted by an organizational change after phosphorylation of LHCII which is not possible at low temperatures. This conformational change is likely to be driven by an increase of the repulsive forces between the complexes after phosphorylation. Such an event should result in a faster diffusion of phospho-LHCII as compared to LHCII. The Monte Carlo simulation at different assumed ratios of $D_{\text{p-LHC}}/D_{\text{LHC}}$ provides information about this effect and the mobility of the other complexes in the appressed thylakoid region. The simulation with a ratio of $D_{\text{p-LHC}}/D_{\text{LHC}}$ as high as 500 generates a biphasic time course with large deviations from the experimental one (Figure 3). The biphasic time course would result from the archipelago effect of slowly

moving complexes which retard the diffusion of one fraction of total phospho-LHCII while the other fraction initially located close to the boundary of the appressed region can escape rapidly to the nonappressed membrane region. The simulation of the experimental data improves at decreasing values of this ratio as indicated by the values of χ^2 in Table II. However, the uncertainty of the experimental data does not allow us to exclude ratios of $D_{p\text{-}LHC}/D_{LHC}$ between 1 and 10 which indicate a diffusion coefficient of phospho-LHCII in the range of $(1.9\text{–}4.4) \times 10^{-12}$ cm^2 s^{-1}. An increase in the diffusion coefficient of LHCII after its phosphorylation would account for the diminished attractive forces between phospho-LHCII and the other complexes in appressed membranes. The repulsive forces of the negative phospho group are likely to induce a local unstacking of appressed membranes. However, in such a model, the diffusion of phospho-LHCII could be obstructed by strong interactions between the surrounding nonphosphorylated complexes. As a result, the diffusion coefficient would not change considerably after phosphorylation, but once having reached the grana border, phospho-LHCII would escape rapidly into the nonappressed membrane region. In general, these results suggest that the appressed region of the thylakoid membrane is a relatively mobile association of complexes and not a rigid assembly of PS II and LHCII. This is also consistent with an efficient repair mechanism after photodestruction of PS II complexes by proteins inserted into the membrane in nonappressed regions [*cf.* Andersson and Styring (1991)].

We have compared two initial distributions of phospho-LHCII, a homogeneous one and a distribution with an enriched concentration of phospho-LHCII near the grana edge, as shown in Figure 1A and Figure 1B, respectively. The fit of our simulations in Figure 4 and the residuals given in Table II are in favor of a more homogeneous distribution of LHCII at the start of diffusion. If phospho-LHCII is almost immobile at 0 °C after its phosphorylation is completed until the start of diffusion by the temperature jump to 20 °C, this result would not be consistent with the localization of the kinase close to the margins as reported (Gal et al., 1990; Yu et al., 1992). However, a more even distribution of the activated kinase as compared to the bulk of the enzyme or differences in the organisms could account for this discrepancy, and more experiments are needed.

Diffusion of Plastoquinone. The diffusion of the integral protein complexes also provides information to understand the obstruction of plastoquinol diffusion. This expands our earlier approach where we considered the protein complexes as immobile relative to plastoquinol (Mitchell et al., 1990). Diffusion of a tracer in the presence of immobile and randomly arranged obstacles is limited if the fraction of the total area covered by the obstacles exceeds the threshold of percolation which is about 0.5 in a two-dimensional lattice (Saxton, 1987). In Figure 5, this fraction is even higher than 0.7. The tracer trapped in finite clusters, i.e., in the domains of Lavergne et al. (1992), could not undergo long-range diffusion. The small size of the clusters at this high density of obstacles is indicated by the black areas in Figure 5A–C. If movement of the obstacles occurs, long-range diffusion of a tracer molecule like plastoquinone is not prevented but only retarded. Such a dynamic model as used in our approach is a more appropriate description of a biological membrane than the static one (Saxton, 1987; Lavergne & Joliot, 1991).

The opening of isolated regions by movement of the complexes enables contact through gaps to other regions. This connectivity between temporarily isolated regions is visualized by the hatched area in Figure 5B,C. After a mean period of 7 walks, an isolated region is found to be adjoined to a neighboring region. This period corresponds to 10–40 ms at a diffusion coefficient of $(1.9\text{–}0.44) \times 10^{-12}$ cm^2 s^{-1} for LHCII (*cf.* eq 2) as determined from the experimental data at a ratio of $D_{p\text{-}LHC}/D_{LHC}$ between 1 and 10 (*cf.* Table II). Thus, the movement of the integral proteins as derived from the subfractionation experiments suggests connections between the isolated lipid areas in the millisecond time scale that are wide enough for passage of plastoquinone. This indicates that the hindrance of plastoquinol diffusion by membrane proteins is not negligible within the rate-limiting time of electron transport of 15 ms (Stiehl & Witt, 1969; Joliot et al., 1992). However, it is not consistent with the suggestion that the plastoquinone pool within the grana membrane is composed of substantially isolated smaller pools which equilibrate slowly within seconds (Joliot et al., 1992).

In conclusion, the present Monte Carlo analysis shows that the membrane cannot be regarded as a solid structure even within the short time scale of the electron-transfer reactions. A fluid lattice with its transient fluctuations is more appropriate to describe the lateral motion even in the appressed grana membrane region where we have found severely restricted movement of the integral complexes.

REFERENCES

Adir, N., Shochat, S., & Ohad, I. (1990) *J. Biol. Chem. 265*, 12563–12568.

Allen, J. F. (1992) *Biochim. Biophys. Acta 1098*, 275–335.

Allen, J. F., Bennett, J., Steinback, K. E., & Arntzen, C. J. (1981) *Nature 291*, 25–29.

Anderson, J. M., & Andersson, B. (1988) *Trends Biochem. Sci. 13*, 351–355.

Andersson, B., & Styring, S. (1991) *Curr. Top. Bioenerg. 16*, 1–81.

Andersson, B., Akerlund, H.-E., & Albertsson, P.-A (1976) *Biochim. Biophys. Acta 423*, 122–132.

Andersson, B., Akerlund, H.-E., Jergil, B., & Larsson, C. (1982) *FEBS Lett. 149*, 181–185.

Armond, P. A., Staehelin, L. A., & Arntzen, C. J. (1977) *J. Cell Biol. 73*, 400–418.

Barber, J. (1982) *Annu. Rev. Plant Physiol. 33*, 261–295.

Binder, K. (1987) in *Application of the Monte Carlo method in statistical physics*, Springer-Verlag, Berlin.

Blackwell, M. F., Gounaris, K., Zara, S., & Barber, J. (1987) *Biophys. J. 51*, 735–744.

Boekema, E. J., Wynn, R. M., & Malkin, R. (1990) *Biochim. Biophys. Acta 1017*, 49–56.

Carlberg, I., Bingsmark, S., Vennigerholz, F., Larsson, U. K., & Andersson, B. (1992) *Biochim. Biophys. Acta 1099*, 111–117.

Cramer, W. A., Furbacher, P. N., Szczepaniak, A., & Tae, G.-S. (1991) *Curr. Top. Bioenerg. 16*, 179–222.

Gal, A., Shahak, Y., Schuster, G., & Ohad, I. (1987) *FEBS Lett. 221*, 205–210.

Gal, A., Hauska, G., Herrmann, R. G., & Ohad, I. (1990) *J. Biol. Chem. 265*, 19742–19746.

Gal, A., Herrmann, R. G., Lottspeich, F., & Ohad, I. (1992) *FEBS Lett. 298*, 33–35.

Gupte, S., Wu, E.-S., Hoechli, L., Hoechli, M., Jacobson, K., Sowers, A. E., & Hackenbrock, C. R. (1984) *Proc. Natl. Acad. Sci. U.S.A. 81*, 2606–2610.

Haehnel, W. (1984) *Annu. Rev. Plant Physiol. 35*, 659–693.

Horton, P., Allen, J. F., Black, M. T., & Bennett, J. (1981) *FEBS Lett. 125*, 193–196.

Hundal, T., Virgin, I., Styring, S., & Andersson, B. (1990) *Biochim. Biophys. Acta 1017*, 235–241.

Joliot, P., Lavergne, J., & Béal, D. (1992) *Biochim. Biophys. Acta 1101*, 1–12.

Kühlbrandt, W., & Wang, D. N. (1991) *Nature 350*, 130–134.

Kyle, D. J., Staehelin, L. A., & Arntzen, C. J. (1983) *Arch. Biochem. Biophys. 222*, 527–541.
Larsson, U. K., & Andersson, B. (1985) *Biochim. Biophys. Acta 809*, 288–290.
Lavergne, J., & Joliot, P. (1991) *Trends Biochem. Sci. 16*, 129–134.
Lavergne, J., Bouchaud, J.-P., & Joliot, P. (1992) *Biochim. Biophys. Acta 1101*, 13–22.
Li, Z., & Scherga, H. A. (1987) *Proc. Natl. Acad. Sci. U.S.A. 84*, 6611–6615.
Mattoo, A. K., & Edelman, M. (1987) *Proc. Natl. Acad. Sci. U.S.A. 84*, 1497–1501.
Metropolis, N., Rosenbluth, A. W., Rosenbluth, M. N., Teller, A. H., & Teller, E. (1953) *J. Chem. Phys. 21*, 1087–1092.
Millner, P. A., & Barber, J. (1984) *FEBS Lett. 169*, 1–6.
Mitchell, R., Spillmann, A., & Haehnel, W. (1990) *Biophys. J. 58*, 1011–1024.
Rubin, B. T., Barber, J., Paillotin, G., Chow, W. S., & Yamamoto, Y. (1981) *Biochim. Biophys. Acta 638*, 69–74.
Saxton, M. J. (1987) *Biophys. J. 52*, 989–997.
Saxton, M. J. (1992) *Biophys. J. 61*, 119–128.
Staehelin, L. A. (1986) *Encycl. Plant Physiol. 19*, 1–84.
Stiehl, H. H., & Witt, H. T. (1969) *Z. Naturforsch. 24*, 1588–1598.
Trissl, H.-W., Breton, J., Deprez, J., & Leibl, W. (1987) *Biochim. Biophys. Acta 893*, 305–319.
Vallon, O., Bulte, L., Dainese, P., Olive, J., Bassi, R., & Wollman, F.-A. (1991) *Proc. Natl. Acad. Sci. U.S.A. 88*, 8262–8266.
Yalovsky, S., Schuster, G., & Nechushtai, R. (1989) *Plant Mol. Biol. 14*, 753–764.
Yu, S.-G., Stefansson, H., & Albertsson, P.-A (1992) in *Research in Photosynthesis* (Murata, N., Ed.) Vol. 1, pp 283–286, Kluwer Academic Publishers, Dordrecht.